Brodogradnja Volume 76 Number 2 (2025) 76201

journal homepage: www.brodogradnja.fsb.hr

Brodogradnja

An International Journal of Naval Architecture and Ocean Engineering for Research and Development

Navigational decision-making method for wide inland waterways with traffic separation scheme navigation system

Luping Xu[1,2], Liwen Huang[1,2], Xingya Zhao[1,2], Jinlai Liu[3], Jiahao Chen[1,2], Kun Zhang[1,2], Yixiong He[1,2]*

[1] *School of Navigation, Wuhan University of Technology, Wuhan 430063, China*
[2] *Hubei Key Laboratory of Inland Shipping Technology, Wuhan 430063, China*
[3] *School of Electrical Engineering, Naval University of Engineering, Wuhan 430014, China*

ARTICLE INFO

Keywords:
Navigation decision-making method
Wide inland waters
Traffic separation systems
Course and speed control system
Digital traffic environment

ABSTRACT

This study utilizes the deep-water channel from the mouth of the Liuhe River to the Jiangyin Bridge in China as a case study to address ship navigation decision-making in wide inland waterways equipped with traffic separation systems. We propose a novel navigation decision-making method based on time-sequence rolling calculations, integrating a digital traffic environment model, collision risk model, and course and speed control techniques. Initially, we innovatively incorporated navigation rules into the quantitative analysis of collision risk based on the behavioral characteristics of ships in the study area. This approach led to the development of a decision-making method capable of adapting to system residual errors and random movements of target ships. Subsequently, a multi-ship navigation decision-making experiment was conducted using available Automatic Identification System (AIS) data for the study area. The results indicate that our method effectively controls ship traffic and ensures timely route tracking in a multi-ship environment within wide inland waters equipped with traffic separation systems, significantly enhancing safety and efficiency.

1. Introduction

With the increasing global demand for transportation, maritime shipping is experiencing notable developments [1]. The density of shipping traffic has increased significantly, making ship safety a paramount concern in the industry [2]. In China, inland water transportation has grown rapidly. As of 2021, the navigable length of inland waterways reached 128,000 km, with a cargo throughput of 4.189 billion tons [3]. However, the increase in transportation volume has also led to a rise in ship collision accidents, making navigation safety a focal issue. Statistical data show that ship collisions account for the largest proportion of inland transportation accidents, with human error being the primary cause [4, 5]. The complex environment and varying ship conditions in inland waters make autonomous navigation without manual intervention

* Corresponding author.
E-mail address: heyixiong7@whut.edu.cn

http://dx.doi.org/10.21278/brod76201
Received 06.09.2024; Received in revised form 07.12.2024; Accepted 09.01.2025;
Available online 14.01.2025
ISSN 0007-215X; eISSN 1845-5859

challenging [6]. However, in waterways such as the Yangtze River section in Jiangsu Province, where channels are wide, water flow is calm, and navigation rules are well-established, the feasibility of navigation assistance and autonomous decision-making methods is high. These technologies are effective in enhancing safety by reducing human error and improving operational automation.

Over the past few decades, collision avoidance methods have evolved significantly. Traditional path generation methods relied on geometric analysis, focusing on metrics like the Distance to the Closest Point of Approach (DCPA) and Time to the Closest Point of Approach (TCPA) [7]. These methods determine feasible steering areas but often overlook collision avoidance rules and ship maneuverability. The Velocity Obstacle (VO) algorithm, an extension of geometric methods, offers real-time obstacle avoidance with fast computation and simplicity [8]. Considering (COLREGs), good seamanship, and maritime practices, based on the ship motion characteristics, [9] proposed a nonlinear VO to obtain higher accuracy in avoiding entry into the ship. A probabilistic VO for real-time collision avoidance was introduced under the uncertainty of target ship (TS) motion [10]. However, in inland waters, the frequent turning of ships prior to encounters creates difficulties in applying VO-based methods [11-13]. A multi-target collision avoidance algorithm based on the Electronic Chart Display and Information System (ECDIS) environmental model realizes collision avoidance between dynamic target vessels and irregular static obstacles [14]; however, it assumes that the target vessel maintains its heading and speed, which is obviously impossible for inland waters. Intelligent optimization techniques have also been developed, including Multi-Population Genetic Algorithms (MGA) [15-17], Ant Colony Optimization, and Particle Swarm Optimization [18], for generating optimal paths. Deep Reinforcement Learning (DRL) [19-22] has been extensively employed in intelligent autonomous systems due to its adaptive and self-learning abilities in complex environments. However, most studies focus on computing collision-free paths without adhering to Collision Regulations (COLREGs) or considering multi-ship scenarios in restricted waters. Inland waters require tailored considerations due to their unique navigational environments. Previous studies have proposed various methods for ship-speed optimization [23], structured decision-making [24], inland river emergency resource allocation problems [25], and decision-making approaches for joining traffic lanes for ships within a TSS [26], but they often overlook multi-ship scenarios, good seamanship, and the impact of unpredictable ship maneuvers.

A review of the literature reveals that the majority of studies on ship collision avoidance focus on open waters with favorable meteorological conditions, while relatively few address inland waters, particularly in complex environments. Current studies do not adequately quantify navigation rules, good seamanship, sources of navigational errors, and the impact of a target ship's uncertain maneuvering on collision-avoidance decisions. To address these gaps, this study develops a situational awareness model for navigation that integrates navigation rules and good seamanship, considers the kinematic constraints of ships, and explores the sources and corrections of navigational errors. A key contribution of this research is the proposal of a navigational decision-making framework based on time-sequential optimization and fast computation. This framework establishes a system for speed and course control, models the state of the target ship, and uses continuously updated dynamic and static environmental information to correct decision-making errors caused by the target ship's uncertain maneuvers. Concentrating on the inland waterway from the Liuhe River to the Jiangyin Bridge (China), this study presents a navigation decision-making method that adheres to navigation rules and embodies the principles of good seamanship. The proposed framework comprises four interconnected modules: situational awareness, situation recognition, speed control, and decision-making, as illustrated in Fig. 1.

The primary contributions of this study are as follows:

(1) A simulation experiment was conducted for a complex environment of multi-vessel coexistence in a wide inland waterway while considering the aspects of navigation rules and good seamanship and accounting for the kinematic constraints of the ships. Notably, the framework was based on the historical automatic identification system (AIS) data available for the study region.

(2) The sources of errors in the control phase of the ship motion were explored, and a navigation error-correction framework based on time-series rolling optimization and fast computation was proposed for addressing the uncertainty of the target ship motion.

The remainder of the paper is organized as follows. Section 2 details the methodology for constructing the environment awareness model. Section 3 introduces the ship motion model, Maneuvering Modeling Group (MMG), and the speed-control system considered in this study. Section 4 describes the navigational decision-making method for TSS water in the wide channel of the Liuhe River. Section 5 presents the multi-ship simulation results and analysis. Finally, Section 6 presents the major conclusions of the study.

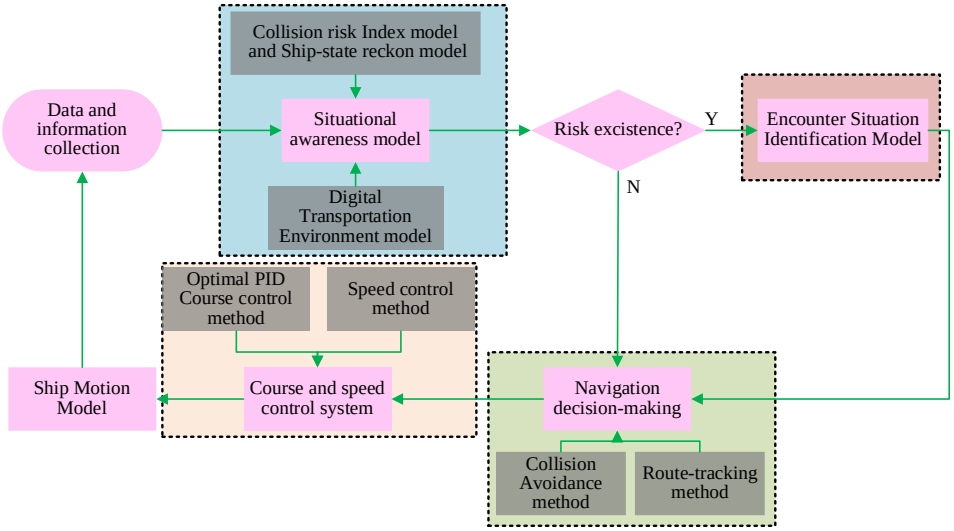

Fig. 1 Flowchart of the navigation decision-making framework proposed in this study

2. Situational awareness model

The situation awareness model for autonomous ship navigation can gather dynamic and static environmental information from the waters surrounding a ship, providing data support for decision-making [27]. Situational awareness primarily consists of two phases: perception and comprehension. The first phase involves sensing; various sensors are employed to gather information from the environment. In the second phase, the collected information is used to assess the current state of the ship. Our study focused predominantly on the comprehension stage for ships, integrating a digitalized traffic environment to determine the risk of collision, thereby providing a foundation for subsequent navigational decisions.

2.1 Digital transportation environment model

Perceiving and extracting environmental information is fundamental to constructing a digital transportation environment for navigation decision-making. This study developed a digital traffic environment model by deconstructing and modeling dynamic and static environmental elements. Static elements, such as channel boundaries, isolation zones, and marking buoys, were extracted using ECDIS tools, while dynamic data, including own-ship (OS), target-ship (TS), and wind current, were processed from shipboard equipment. Combining these, a comprehensive digital environment was established to support navigational decisions [8].

Table 1. Classification of objects

Type of environmental element	Elementary models	Element status
Buoys, surface (reefs)	Punctiform	Static
Shoal, shoreline	Polygonal	Static
Conventional motorized ships	Ordinary motorized ships	Dynamic
Tug and trawl fishing ship	Striped	Dynamic
Maneuvering limited ships, uncontrolled ships	Circular	Dynamic
Non-motorized ship	Punctiform	Dynamic

Elements outside the navigational subchannels were classified into point, circular, bar, and polygonal object models. The specific classifications of the digital transportation environment are listed in Table 1.

A digital transportation environment model was applied to the study area (Figure 2).

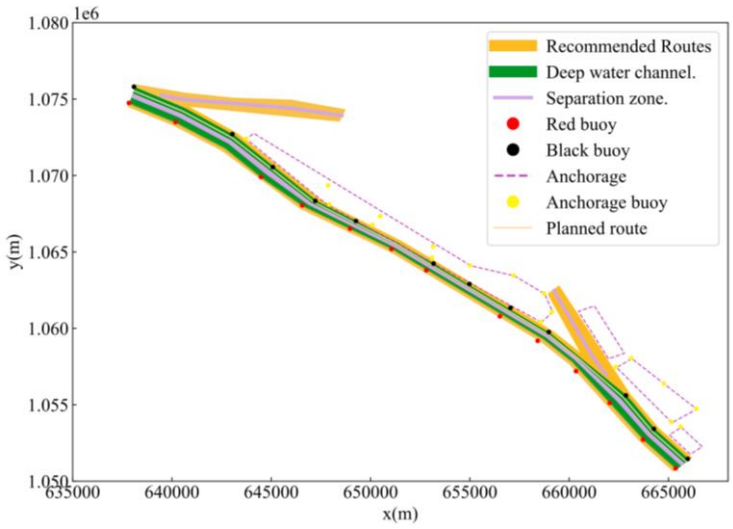

Fig. 2 Digital traffic environment from LiuHe River to Jiangyin Bridge (China)

2.2 Ship collision-risk index model

2.2.1 Ship-state reckon method

Contrary to open waters, due to the complexity of the environment and traffic flow [28], the positions of ships in the waters of a traffic separation system are constrained by environmental constraints of the channel and navigation rules. Considering that ships generally continue along the fairway when their tracks align with the recommended traffic-flow direction is essential to estimate the positions of the target ships in real-time. If there is a significant difference between the ship's track and fairway direction, or if the ship is outside the fairway, the ship's position is estimated based on its current velocity vector. If a ship deviates from the planned route, owing to evasive actions or other operations, it is advisable to adjust the course as soon as conditions permit it, to resume sailing in the same direction as the recommended traffic flow (see Figure 3).

When ships are both with and against the traffic flow direction, the position of TS can be calculated using Eqs. (1) and (2).

(1) When TS was outside the TSS, the dead node was utilized to determine its position relative to the speed vector, as shown in Eq. (1):

$$\begin{cases} x_t = x_0 + v \times t \times \sin(TC) \\ y_t = y_0 + v \times t \times \cos(TC) \end{cases} \tag{1}$$

where (x_t, y_t) denotes the position of the TS at time t. (x_0, y_0) represents the current position of the TS; v and TC denote the speed and course of the TS, respectively.

(2) When the TS was inside the TSS, the dead-reckoning method outlined in Eq. (2):

$$\begin{cases} \begin{cases} x = x_0 + v \times t \times \sin(TC) \\ y = y_0 + v \times t \times \cos(TC) \end{cases} & t \in \left[0, t_j\right) \\ \begin{cases} x = x_1 + v \times \left(t - t_j\right) \times \sin\left(\alpha_{i+1}\right) \\ y = y_1 + v \times \left(t - t_j\right) \times \cos\left(\alpha_{i+1}\right) \end{cases} & t \geq t_j \end{cases} \tag{2}$$

where α_{i+1} represents the recommended traffic flow direction for the next segment, (x_1, y_1) indicates the position of the TS upon arrival at the next segment, and t_j is the time indicating the arrival of the TS at the next segment.

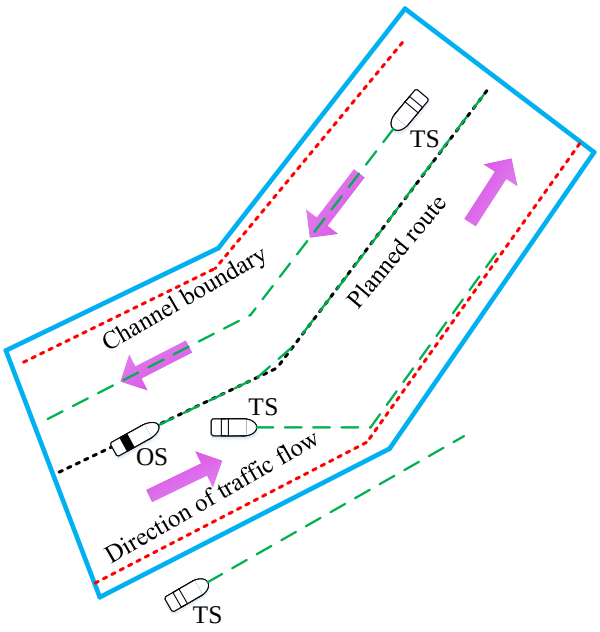

Fig. 3 Dead reckoning of ship position

If the TS is within the traffic lane, then Eq. (2) can be used to determine the vehicle's position during navigation, in accordance with the recommended traffic flow direction, whereas Eq. (1) is used when it is not.

2.2.2 Ship domain model

The ship domain is utilized to assess collision risk. We chose the eccentric elliptic ship domain model as it accounts for the specific requirements related to competent seamanship and the TSS COLREGs (Figure 4).

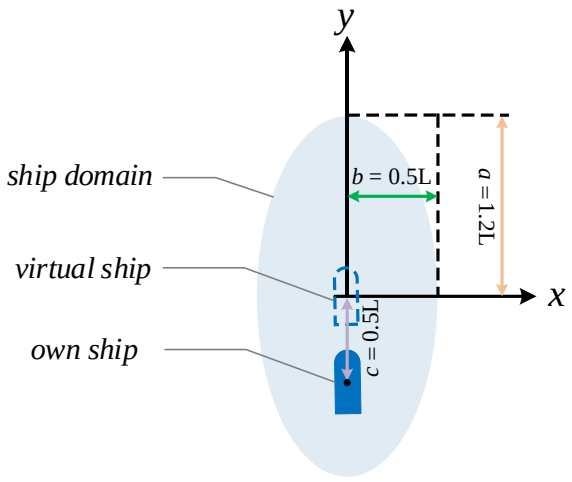

Fig. 4 Illustration of the ship domain model used in this study; *L* is the length of the own-ship (OS)

This model was chosen for the TSS watershed based on the following considerations:

(1) Ships require greater safety clearance in the fore-and-aft direction than port and starboard due to larger distance variations between bow and stern during maneuvering.

(2) In inland TSS waters, avoiding collisions at the bow or stern is more challenging, especially in overtaking scenarios, necessitating greater safe distances at the bow.

(3) In the waters of the Chengshanjiao traffic separation system, the elliptical ship field set [29] has a long axis that is five times the length of the ship and a short axis that is two times the length of the ship. However, this method used only for sea navigation. In general, the traffic flow density is higher in inland waterways. Based on discussions with experienced captains who have navigated ships in the Yangtze River inland waterways, we set the ship field long and short axes to 1.2 and 0.5 times the length of the ship, respectively.

2.2.3 Collision risk index (CRI) model

When navigating a temporally varying and complex inland waterway environment, multiple target ships may be encountered, posing the risk of collision with the OS; notably, the situations encountered may vary. Therefore, a CRI model was introduced to quantify the collision risk spatiotemporally and prioritize the collision-avoidance actions according to the magnitude of the CRI.

The CRI was determined by analyzing the correlation between the maneuvering characteristics, positions, and movements of the two ships. Importantly, the CRI represents a numerical value that indicates the level of collision risk and the urgency of collision-avoidance actions [30]. It combines both the time collision risk index (TCRI) and the space collision risk index (SCRI), as shown in Eq. (3):

$$u = u_s \cdot u_t \tag{3}$$

where u, u_s, and u_t denote the CRI, SCRI, and TCRI, respectively.

In this paper, the threshold value for u is set at greater than 0.2. Additionally, the OS, as the give-way vessel, can also take proactive measures to avoid a collision. The associated collision risk is illustrated in Figure 5.

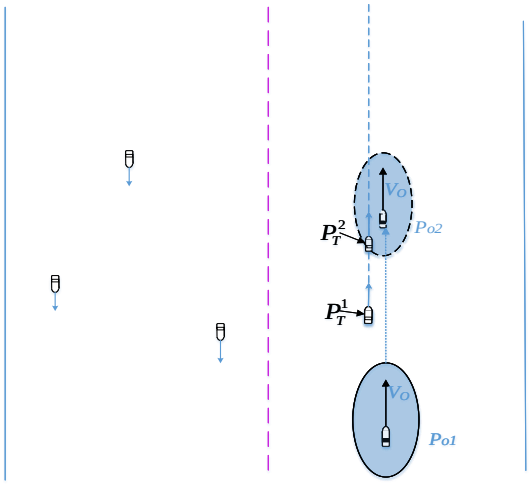

Fig. 5 Collision-risk determination

3. Ship course and speed control system

A ship generally has six degrees of freedom; however, this study focuses on the control of the ship's planar motion, while assuming that the effects produced by the ship's transverse rocking, longitudinal rocking, and pendulum swinging are negligible. In this study, the ship course and speed control system was established by constructing a three-degree-of-freedom MMG model, while combining speed and course control methods.

3.1 Ship maneuvering motion model

In recent years, different mathematical models of ship maneuvering for displacement have been proposed [31]. The motion of a ship generally has six degrees of freedom [32]; however, this study focuses on the control of the ship's planar motion, while assuming that the effects produced by transverse rocking, longitudinal rocking, and pendulum swing are negligible. Considering external environmental factors, such as

wind, waves, and current interference, we established the ship maneuvering motion model with the MMG algorithm, as shown in Eq. (4):

$$\begin{cases} \left(m+m_y\right)\dot{v}+\left(m+m_x\right)ur = Y_H+Y_P+Y_R+Y_{\text{wind}}+Y_{\text{wave}} \\ \left(m+m_x\right)\dot{u}-\left(m+m_y\right)vr = X_H+X_P+X_R+X_{\text{wind}}+X_{\text{wave}} \\ \left(I_{zz}+J_{zz}\right)\dot{r} = N_H+N_R+N_P+N_{\text{wind}}+N_{\text{wave}} \end{cases} \tag{4}$$

where m, m_y, and m_y represent the mass of the ship and the additional mass generated along the x and y axes, respectively. I_{zz} and J_{zz} represent the moment of inertia of the ship and additional moment of inertia, respectively. The variables u, v, and r, along with their derivatives, correspond to the ship's velocity and acceleration in the x and y axes, as well as their angular velocity and acceleration. The symbols X, Y, and N denote the forces and moments exerted on the hull, oar, and rudder along the x and y axes, respectively. The subscripts H, P, R, wind, and wave indicate the effects of the wind and water flow on the hull, oar, and rudder, respectively. The relevant parameters were calculated as described by [33] and the formula for solving the wind-flow problem can be found in [34].

A Panamanian bulk carrier with a maximum load of 76,000 ton was selected as the OS native ship for modeling; the ship parameters are listed in Table 2.

Table 2. Ship parameters considered in this study

Parameter	Ship data
Name	HUANG YANG DREAM
Displacement	90000 x 10 kg
Length	225 m
Breadth	32.5 m
Draft	14.5 m
Density of water	1000 kg/m
RPM (sea speed)	90 r/min
C_b	0.8715
Acreage of rudder	56.88 m²
Propeller advance	4.738 m

3.2 Ship course control method

Ship course-keeping is crucial for navigation efficiency and safety [35, 36]. PID is the most commonly used control method within the engineering control field. The rudder angle is adjusted according to the deviation (E) between the actual heading and the desired heading and its rate of change (EC), and the vessel's heading is controlled by limiting the rudder angle to [-35°, 35°] through a limiting mechanism that ensures a stable heading (see Figure 6).

The control law of rudder angle is shown in Eq. (4):

$$\delta(t) = K_P\left[E+\frac{1}{T_i}\int_0^t E\mathrm{d}t+T_d\cdot EC\right] \tag{5}$$

where K_P, T_i, and T_d denote the proportional, integral, and derivative parameters, respectively. E is the system error and EC is the rate of change of error; $\delta(t)$ is the output of the PID.

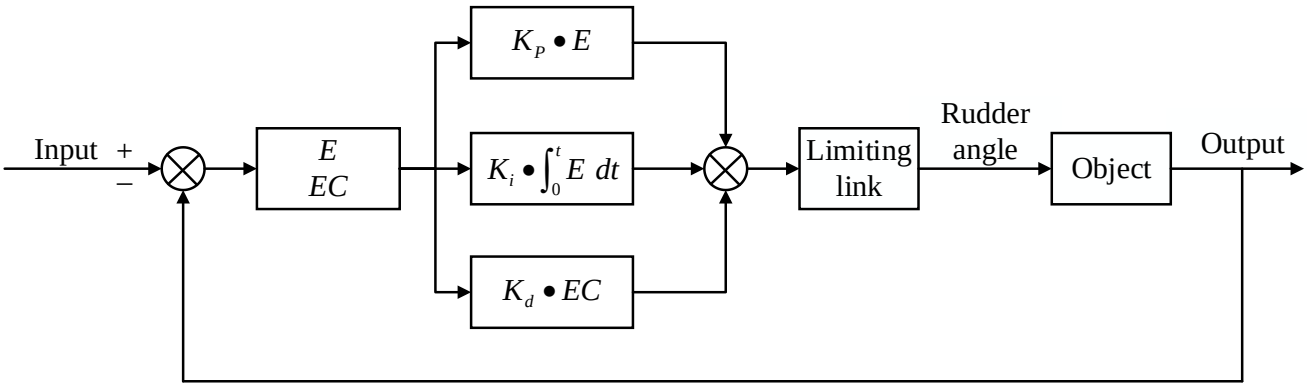

Fig. 6 Principle of proportional integral derivative (PID) automatic rudder

Conventional PID parameters are generally fixed and cannot be adjusted adaptively according to the environment. By introducing the optimal control theory, the adaptive adjustment of PID parameters is realized.

To obtain the ship maneuverability indices K and T, Eq. (4) was transformed through Laplace transformation, to obtain the second-order response model, as shown in Eq. (6):

$$\begin{cases} \left(m+m_x\right)su(s)=\left(X_r-\left(m+m_y\right)v_0\right)r(s)+X_u v(s)+X_\delta(s) \\ \left(I_{zz}+J_{zz}\right)sr(s)=N_u(s)+N_r r(s)+N_\delta\delta(s) \end{cases} \tag{6}$$

After the inverse Laplace transformation, the relationship among the yaw rate, lateral acceleration, and rudder angle in the frequency domain can be transformed into a time-domain equation, as shown in Eq (7):

$$\begin{cases} T_1T_2\ddot{r}+\left(T_1+T_2\right)\dot{r}+r=K\left(\delta+T_3\dot{\delta}\right) \\ T_1T_2\ddot{u}+\left(T_1+T_2\right)\dot{u}+u=K_u\left(\delta+T_{3u}\dot{\delta}\right) \end{cases} \tag{7}$$

where K, T_1, T_2, and T_3 are the ship maneuverability indices, and $T=T_1+T_2-T_3$.

Thus, the ship maneuverability index was calculated from the hydrodynamic derivative in the MMG model, an expression related to the ship speed. Thus, the ship maneuverability index is ultimately a function of the ship speed (v).

The selection of a performance optimization function that considers both course maintenance and fuel savings is expressed in Eq (8):

$$J=1/2(\varphi_e^2+\lambda\delta^2) \tag{8}$$

where φ_e is the course deviation, and λ is a weighting factor whose value is related to the magnitude of wind speed. The relationship between λ and wind speed is shown in [37].

To minimize the value of the quadratic performance optimization function in Eq. (9), the control law for the rudder angle was solved using the linear quadratic nonstationary output theory:

$$\delta=\left[\frac{1}{\sqrt{\lambda}}\frac{1}{K}\left(1-\sqrt{1+\frac{2KT}{\lambda}}\right)\right]\left[\frac{E}{EC}\right] \tag{9}$$

Then, k_p, k_d, and K_i were calculated using Eqs. (10-12):

$$K_p=\frac{1}{\sqrt{\lambda}} \tag{10}$$

$$K_d=\frac{1}{K}\left(1-\sqrt{1+\frac{2KT}{\lambda}}\right) \tag{11}$$

$$K_i = \frac{1}{10}\sqrt{\frac{K}{T\lambda}} \tag{12}$$

The course-adaptive optimal control was realized based on the PID parameters derived in this study. The adaptive optimal course control was implemented based on the aforementioned PID parameters. The specific principles are illustrated in Figure 7.

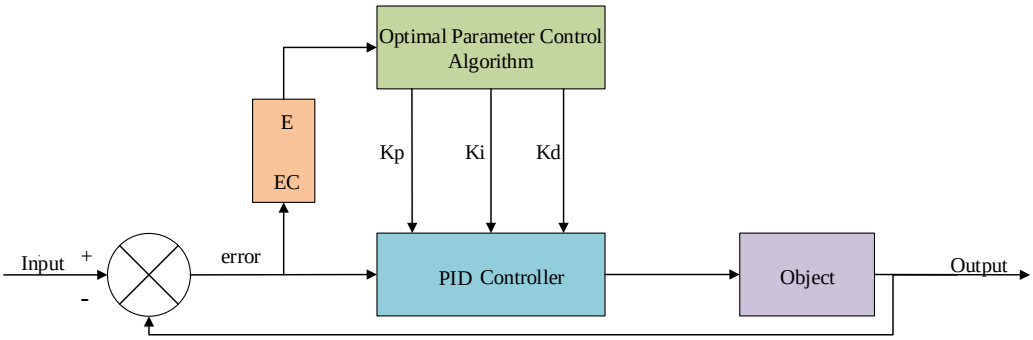

Fig. 7 Adaptive optimal proportional integral derivative (PID) controller

We compared the performance of the optimal PID controller designed in this study with that of a conventional PID controller for a Panamanian bulk carrier (with a maximum full load of 76,000 tons) (Table 2). The optimal PID controller simulated the ship's course using the established MMG model. The range of the course change was set between [-30°, 30°], with the λ value set to 0.1, and a step size of 1 second. Movements to the left and right were considered negative and positive, respectively. Figure 8 presents a comparison of the simulation results for both the optimal and conventional PID controls. Additionally, the variations in velocity as a function of K and T are illustrated in Figure 8.

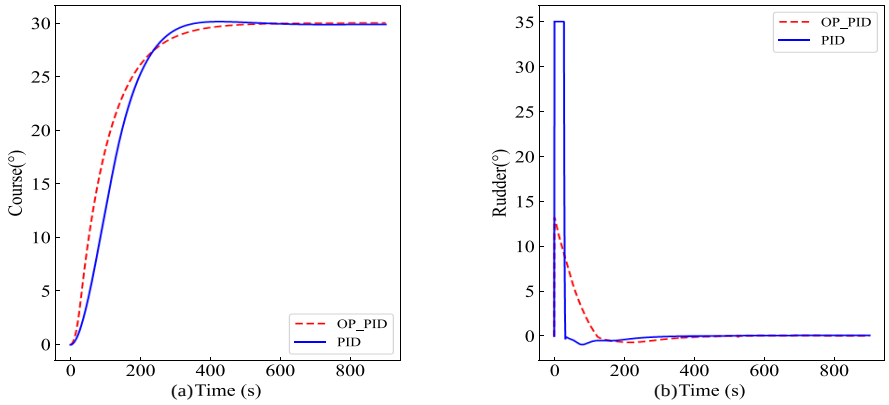

Fig. 8 Simulation of course control based on the (a) optimal and (b) conventional proportional integral derivative (PID) controls

The following conclusions were drawn from the course and rudder angle curves shown in Figure 8:

(1) As shown in Figure 8a, when the ship-course changes were minor, the optimal PID control algorithm responded faster, overshot less, and converged more quickly than the traditional PID control algorithm.

(2) As shown in Figure 8b, the optimal PID control algorithm gently managed the rudder-angle changes and responded more quickly, thereby enhancing the steering control of the ship. This may contribute to improved maneuvering performance and navigation safety.

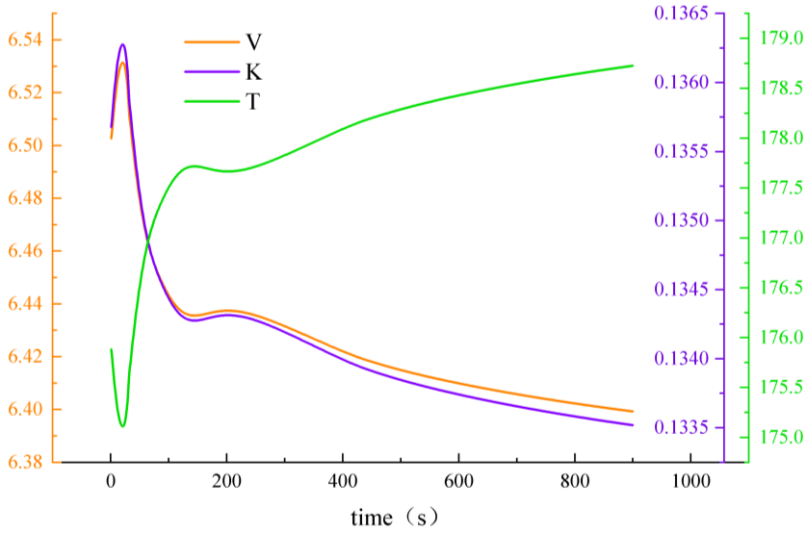

Fig. 9 Variations in the curves of *K* and *T* with speed

Figure 9 portrays the change process of the ship speed and the *K* and *T* values during ship reorientation in the optimal PID model; the figure verifies that the proposed course-control method could adjust the PID parameters in real time, according to the ship speed.

3.3 Ship speed control method

In general, ships achieve speed variations by adjusting the propeller rotation speed. In practice, minor changes in the propeller rotational speed have negligible impact on the effectiveness of collision avoidance. Therefore, selecting a graded vehicle bell to issue speed commands is preferred. Considering the speed limits specified in navigation rules, only the forward speed of the ship must be considered. Table 3 portrays the experimental simulation of the ship's telegraph and matching speed.

Table 3. Telegraph tachometer

Telegraph	Rotation (r/min)	Speed (kn)
Sea speed	93	14
Full ahead	85	13
Half ahead	70	10.5
Slow ahead	48	5
Dead slow ahead	35	3

If the vehicle command was issued at time t_1 and the time to complete the speed change was t_2, with propeller speeds before and after the speed change denoted as P_1 and P_2, respectively, the propeller speed at time t can be expressed as follows:

$$P_t = \begin{cases} P_1, & t < t_1 \\ P_2, & t > t_2 \\ P_1 + (t - t_1) \times k, t_1 < t < t_2, & P_1 < P_2 \\ P_1 - (t - t_1) \times k, t_1 < t < t_2, & P_1 > P \end{cases} \tag{13}$$

where *k* represents the rate of change of propeller speed, which, according to the length of the ship's wheel, was considered to be 0.25 r/s (based on the empirical data).

Based on the MMG model constructed from the ship's parameter information shown in Tables 2 and 3, we determined the true and modeled speeds of the ship (shown in Figure 10).

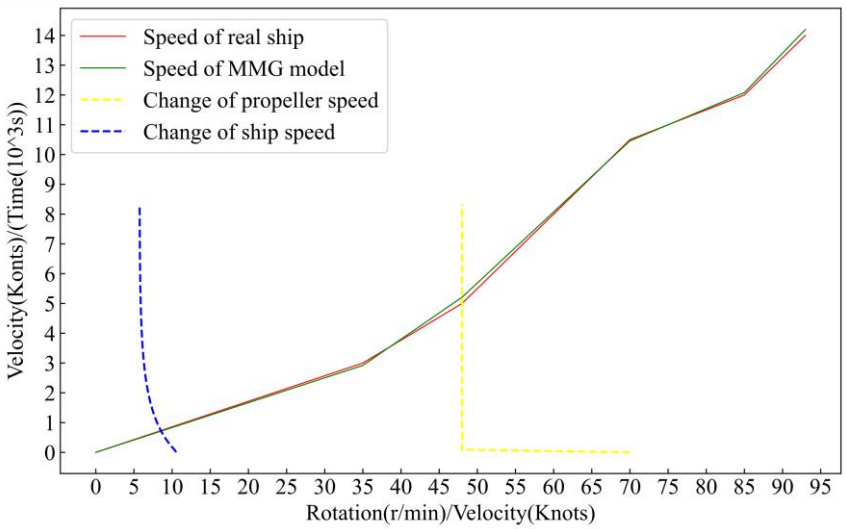

Fig. 10 Comparison of ship speed to the Maneuvering Modeling Group (MMG) model's speed

As shown in Figure 10, the red and green lines represent the actual ship speed and the ship speed according to the MMG model, respectively. The difference between the two is insignificant, and the accuracy satisfies the requirements for ship maneuverability predictions. The blue and yellow lines denote the changes in the ship and propeller speeds during the deceleration of the experimentally simulated ship from full to half speed, showing obvious nonlinear changes.

4. Navigation decision-making method in wide inland waterways

In open seawater, course alteration is the most effective action for collision-avoidance. However, in inland waters, owing to the channel-width and water-depth restrictions, single steering cannot ensure the safe navigation. Therefore, in this study, we considered the scenarios of ships navigating inland waters and proposed a navigation decision-making method based on navigation rules, channel environment, and good seamanship. This method involves the alteration of course, change in speed, or a combination of both.

In a temporally varying navigational environment of wide inland waterways, the information of target ships and environmental information are acquired in real time, with the preferred step-size being 1s. By analyzing the sources and systematic errors, we constructed a navigation decision-making framework based on time-sequence scrolling that is continuously compensated for, with updated errors. Furthermore, we searched for the optimal decision scheme at the current moment, and executed it cyclically.

4.1 Collision-avoidance decision-making methods

4.1.1 Encounter-situation identification model

Ships should take appropriate collision-avoidance actions in different encounter situations, as stipulated by the navigation rules. Therefore, we proposed a method for identifying ship encounter situations consistent with these rules and good seamanship for the characteristics of inland TSS waters.

In addition to stipulating the responsibilities and obligations of the two ships in collision-avoidance actions when there is a danger of collision, the navigation also included special provisions for the mouth of a branching estuary. Eq (14) can be used to determine whether a ship is in a branching estuary (see Figure 11):

$$\left.\begin{aligned} o &= (X_k^2 - X_k^3)\times(Y_t^0 - Y_k^3) - (Y_k^2 - Y_k^3)\times(X_t^0 - X_k^3) \\ p &= (X_k^1 - X_k^4)\times(Y_t^0 - Y4) - (Y_k^1 - Y_k^4)\times(X_t^0 - X_k^4) \\ q &= (X_k^2 - X_k^1)\times(Y_t^0 - Y_k^1) - (Y_k^2 - Y_k^1)\times(X_t^0 - X_k^1) \\ r &= (X_k^3 - X_k^2)\times(Y_t^0 - Y_k^2) - (Y_k^3 - Y_k^2)\times(X_t^0 - X_k^2) \end{aligned}\right\} \quad (14)$$

where (X_k^i, Y_k^i) denote the coordinates of the kth section of the mouth of the branching estuary; (X_t^0, Y_t^0) denotes the OS position at time t; o, p, q, and r denote the judgment coefficients. Notably, TS is considered to be in the mouth section of the branching estuary only if *o*, *p*, *q*, and *r* are simultaneously greater or less than 0.

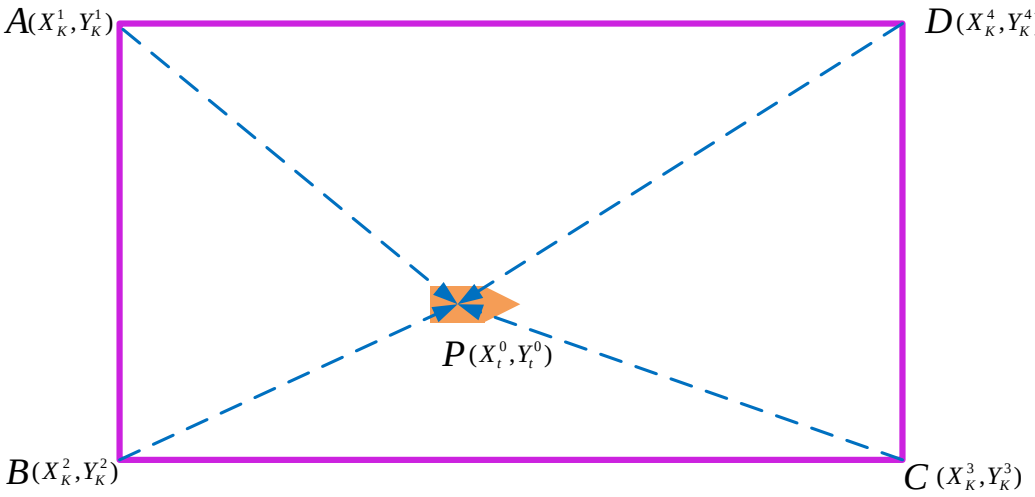

Fig. 11 Diagram of the segment considered in this study

To clarify the encounter situations between ships, we developed a method to assess ship encounters by analyzing navigation rules and principles of good seamanship, with a focus on the difference between the traffic flow direction and the ship's course. An encounter-situation identification model was also created for the study area. Using this model, the type of encounter between the OS and TS that demonstrated the highest CRI was identified (see Table 4).

Table 4. Encounter situation identification model

Type	Situation	Conditions
Danger	Overtaking	$\lvert\varphi_t^0 - \varphi_m^0\rvert \le 5^\circ, \lvert\varphi_t^i - \varphi_n^i\rvert \le 5^\circ, m = n$
	Head-on	$\lvert\varphi_t^0 - \varphi_m^0\rvert \le 5^\circ, \lvert\varphi_t^i - \varphi_n^i\rvert \le 5^\circ, m \ne n$
	Traverse	$\lvert\varphi_t^0 - \varphi_m^0\rvert \le 5^\circ, 85^\circ \le \lvert\varphi_t^i - \varphi_n^i\rvert \le 95^\circ$
	Crossing	Not constituting overtaking, head-on, Branching Estuary, Traverse situations
	Branching Estuary	$\lvert\varphi_t^i - \varphi_n^i\rvert \le 5^\circ$
No Danger	/	

When danger exists, the courses of the OS and TS are φ_t^0 and φ_t^i, respectively. The main streams of the corresponding ship's section are φ_m^0 and φ_n^i, respectively, where m and n represent the numbers of upward and downward shipping routes, respectively. The process of identification of the encounter situation is similar to that shown in Figure 12.

As shown in Figure 12, if the OS tracks the planned route, it will be in danger with TS1, TS2, TS4, and TS5, identified as overtake, crossing, branching estuary, and traverse situations, respectively, according to the encounter identification model.

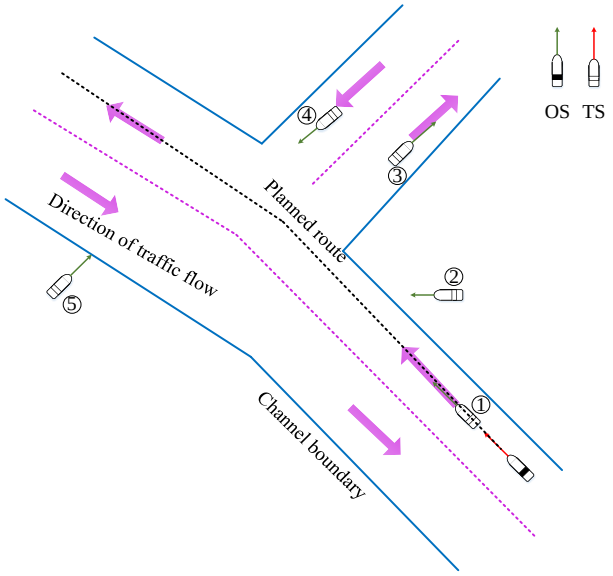

Fig. 12 Encounter-situation identification. Abbreviations: own-ship (OS), target-ship (TS)

4.1.2 Collision-avoidance actions: Changing speed and altering course

The OS can employ different maneuvers, such as altering the course, altering the speed, or combining both, to avoid collisions. If there is a risk of collision, the TS with the highest collision risk at that moment can be calculated. The calculation involves determining the alteration in the course angle and speed adjustment. The priority sequence for the collision avoidance actions is as follows: altering the course, altering the speed, and combining both. The steps for determining this are as follows:

(1) Relying solely on course alterations: According to the navigation rules, when relying solely on the alteration of the course, all feasible courses of the OS can be represented as shown in Eq. (15):

$$C_{\text{aim}} = C_0 \pm \alpha, 1^\circ \le \alpha \le 30^\circ \tag{15}$$

where C_{aim} is the target course, and C_0 is the initial course; α is the reorientation angle, ranging from $1^\circ - 30^\circ$.

C_{aim} to the course and speed control system can be input and whether the target ship and other obstructions (outer boundaries of the channel, beacons, shoals, etc.) would enter the ship's field can be verified. At this time, C_{aim} represents the target course for the sole alteration of course, and α is the minimum reorientation angle. If not all reorientation angles are feasible, Scheme (2) is adopted. If the OS domain reaches the TSS channel boundary line, the course is updated in the direction of the channel boundary line for the current segment.

(2) Relying solely on speed changes: Based on the performance of the main engine, the achievable RPM of the ship can be expressed using Eq. (16):

$$N_{\text{aim}} = N_0 \pm \Delta N, N_{\text{aim}} \in [N_s, N_F] \tag{16}$$

The target RPM N_{aim} and target course C_{aim} from the route-tracking method are input into the course and speed control system. Whether each RPM setting is feasible for evasion is gradually verified. The plan with the smallest RPM adjustment magnitude is considered to be the optimal evasion plan, solely relying on speed adjustment. If none of the RPM settings are feasible, Scheme (3) is adopted.

(3) Alteration of course and speed: Based on the C_{aim} and propeller speed N_{aim} of the OS listed in (1) and (2), the RPM setting is incrementally adjusted starting from the smallest alteration angle. C_{aim} and N_{aim} are input into the course and speed control system, sequentially verifying whether the TS and other obstacles could enter the OS domain. The combination of the smallest alteration angle and RPM adjustment is considered the optimal evasion plan. Manual intervention is required if an effective plan is not established.

4.1.3 Collision-avoidance decision-making methods for wide inland waterways

For motorized ships operating under an OS in the direction of traffic flow in the study waters, the following conditions must be met:

(1) Ships must travel within the prescribed navigable subchannels or lanes

(2) Ships entering and exiting the mouths of branching estuaries, tributaries, and dedicated waterways should actively avoid traveling normally within the prescribed navigable subchannels and recommended routes

(3) Large ships with low speeds in navigable subchannels should travel along the right edge of the subchannels as far as possible and enter the recommended routes for navigation if safety is guaranteed

(4) Compliance with rules for Preventing Collisions on Inland Waterways of the People's Republic of China

To determine the encounter situation, we introduced the situation recognition model, and the avoidance relationship between the two motorized ships was determined according to the encounter situation, as shown in Figure 13.

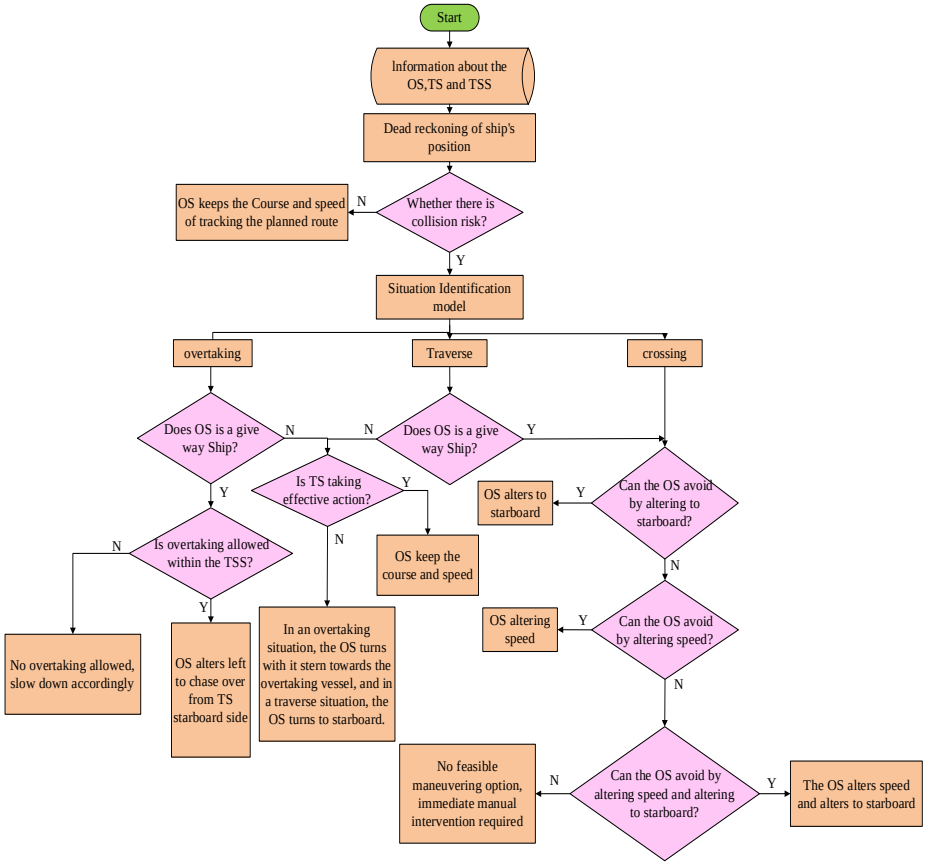

Fig. 13 Flowchart portraying collision-avoidance process for wide inland waterways

4.2 Route-tracking decision-making method

After addressing the problem of ships deviating from their routes and tracking their routes after avoidance was completed, a line-of-sight (LOS) guidance algorithm was introduced (see Figure 14). The ship was controlled to sail along the planned route by deriving its target course, while tracking the desired course point. To calculate the course of the ship, the y axis of the coordinate system was in the north direction, and x axis was in the east direction; the ship course was the angle between the bow and north directions.

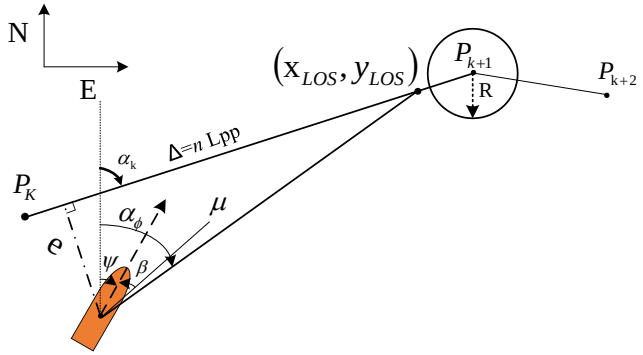

Fig. 14 Schematic of line-of-sight (LOS) guidance

As shown in Figure 14, the desired course point $P_{LOS} = (x_{LOS}, y_{LOS})^T$ was at a distance of nL_{PP} from the projection point of the ship on the desired track, where L_{PP} is the length of the ship, and n ranges from 2 to 5. Δ represents the ship's visibility distance. The desired course angle is expressed as Eq (17):

$$\alpha_\phi = \alpha_k + \arctan\left(\frac{-e}{\Delta}\right) \tag{17}$$

where α_ϕ represents the desired course angle of the ship, e denotes the lateral tracking error of the ship, and α_k is the angle between the true north direction of the geographic coordinate system and the desired track line. Note that $P_k P_{k+1}$, ψ represents the current course angle of the ship, and R is the ship's advance turning distance. The course angle deviation is denoted by ψ_e.

If the ship position coordinate is (x_0, y_0), the desired course point of tracking at this time is $P_k = [x_k, y_k]^T$, and the desired course angle is α_ϕ, as obtained from the aforementioned guidance algorithm; thus, the ship's course angle deviation will be: $\psi_e = \alpha_\phi - \psi$. Note that ψ_e can be transmitted to the adaptive optimal course control system, which will compute the corresponding rudder angle δ, and transmit it to the ship motion model. Simultaneously, the ship course and position are updated and fed back to the guidance algorithm, relying on a closed-loop data iteration to ensure that the ship tracks the course stably.

The principle of the tracking method is illustrated in Figure 15.

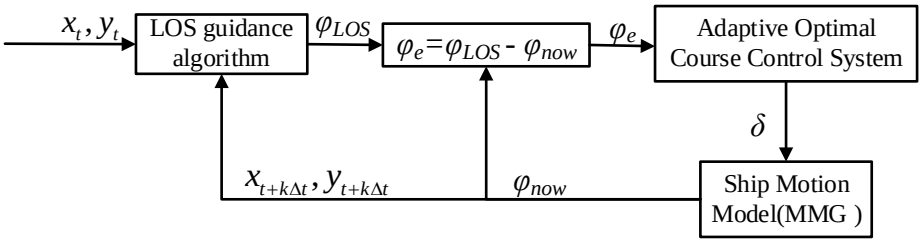

Fig. 15 Principle of path tracking method

In Figure 15, (x_t, y_t) denotes the OS position at moment t and $(x_{t+k\Delta t}, y_{t+k\Delta t})$ denotes the OS position at moment $t + k\Delta t$, where k is a positive integer and Δt is the step size. When ψ_e tends to 0, the ship sails toward the target course point. When the ship is less than a set distance R from the next desired course point, it automatically switches to track the course point.

The maneuvering scheme can be solved at any t moment, and the OS can be avoided. Simultaneously, the target course can be calculated according to the course-tracking method and dead reckoning of the ship's position. If there is no danger, the course-tracking program is executed. The specific timing of the course tracking is solved using the method shown in Figure 16.

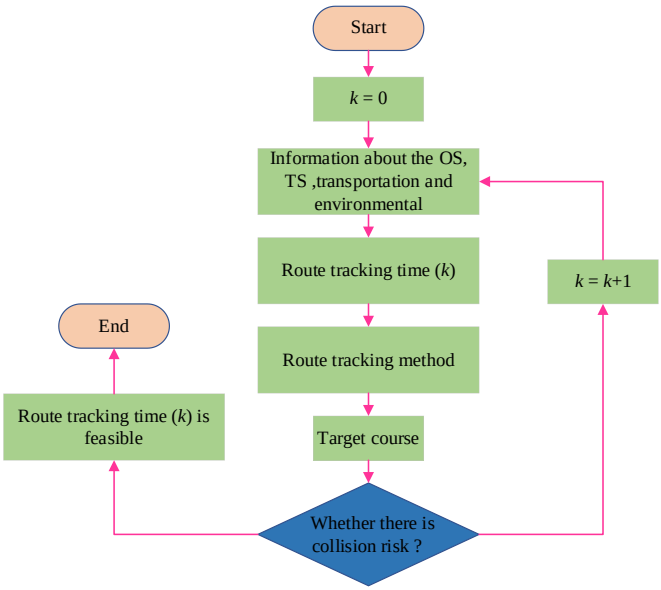

Fig. 16 Calculating the time to route tracking

4.3 Navigation decision-making method based on the error correction

In autonomous ship navigation, environment sensing is the key to navigation decision-making. Environmental sensing monitors the motion states of dynamic and static objects, to provide basic information for decision-making; however, the errors in sensing, uncertainties in the ship's motion model, and variations in control parameters can lead to errors. These errors can be reduced by selecting suitable mathematical models, improving sensor accuracy, and optimizing controller parameters. Notably, minor errors will still exist. These errors are defined as residual errors and can be compensated for by designing an adaptive feedback correction system.

The adaptive navigation decision-making system calculates the navigation decision of time t based on the navigation information of $t + \Delta t$ times, to ensure the safety of navigation within the time of Δt. The decision-making within each Δt cycle is updated according to the real-time navigation information, to compensate for the decision error in Δt. Note that Δt is maintained in a suitable range. Thus, even if errors are present, they can be maintained within a controllable range through continuous updates.

Based on the aforementioned concepts, a time-sequenced rolling adaptive navigation decision framework was constructed in this study. Information on the ship and traffic environment was the input, and the time-sequence maneuvering scheme of the ship was the output. We acquired the dynamic and static target information with the step size Δt, with Δt being 1s, to judge its motion state in real-time, analyze the navigation posture, conduct feedback regulation, and execute the maneuvering scheme. The decision-making process is shown in Figure 17, with the following steps:

(1) Construct a digital transportation environment.

(2) Input information about the target ship, other object markers, navigation channel, and movement state of the ship.

(3) Based on the dead-reckoning method, the positions of the OS and TS are estimated, collision risks are assessed, and a maneuvering scheme under the navigation rules is determined. If no risk is detected, the route tracking method is used to calculate the target course and speed, while inputting these data into the course speed control, and assessing the safety of route tracking. Whether safe or not, execute the route-tracking program; otherwise, execute the current program.

(4) Update information and repeat (2) to (4).

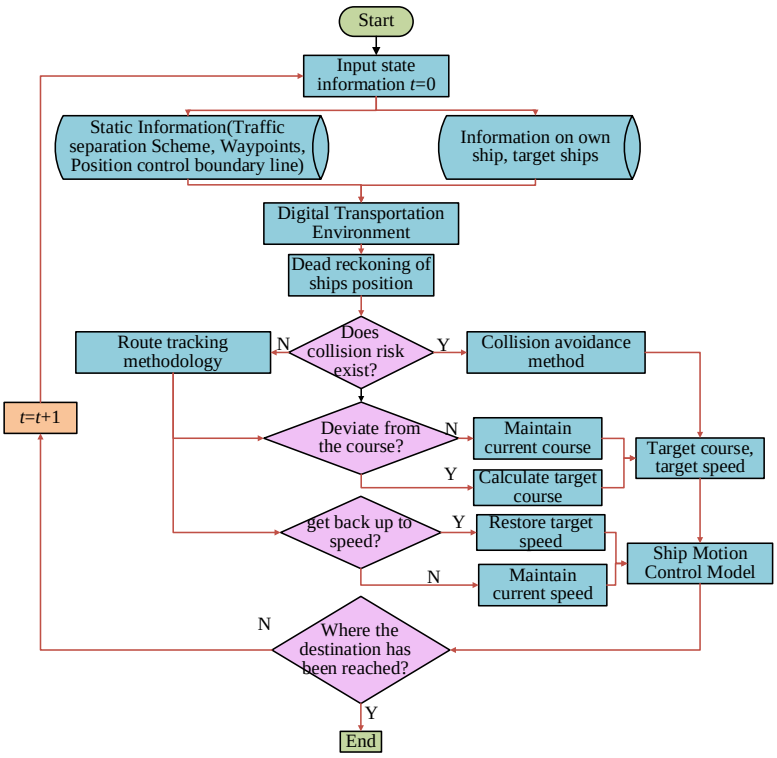

Fig. 17 Decision-making framework for navigation

The steps were based on the time-sequence rolling calculation method, which rapidly updated the navigation information and compensated for the effects of residual errors on the maneuvering plan. In practice, if a ship does not comply with the navigation rules, the OS will immediately update its decision-making scheme based on its movements, until safety is assured.

5. Case study

A Python-integrated development environment was used for the simulations. In the experiment, (22°5'.27N, 114°17'.54E) was considered as the origin of *XOY*.

5.1 Environment setup

Wind, waves, currents, and other external meteorological conditions directly affect the tracking accuracy of routes and collision-avoidance decision-making programs. The real-time wind, wave, and current data of the section from the Liuhe River to the Jiangyin Bridge from 1600 to 1800 on September 17, 2023, are shown in Table 5. Considering that the water environment was relatively closed and the draught and displacement of the ship were relatively large in deep-water waterways, the impact of waves on the ship's voyage in the study area was relatively small, and thus, the effects of waves were not considered.

Table 5. Simulation environment

\	Wind	Wind Direction	Current	Current Direction
Unit	Speed (m/s)	Direction (°)	Speed (m/s)	Direction (°)
Data	2.1	313	0.2	150

To verify the feasibility of the proposed ship navigation decision-making method, we used real-time AIS data of the section from the Liuhe River to the Jiangyin Bridge from moment of 1400 to 1600 on September 17, 2023, to conduct simulation experiments (Figure 18).In order to ensure the completeness and usability of the ship trajectory data and provide reliable data for subsequent studies, the missing data and short-range sparse trajectories are repaired by linear interpolation, which is not the main task of this study, and the specific method can be referred to [38].

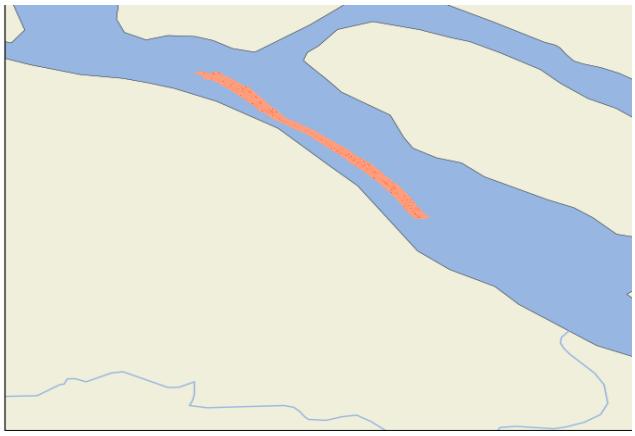

Fig. 18 Traffic flow for selected time periods

5.2 Simulation scenario

The environmental settings used in the simulation experiment are listed in Table 6. The OS position was (121°19.224′E, 31°33.759′N), OS course was 319°, and velocity was 6.5 m/s. Simulation experiments were conducted using processed AIS data indexed by time, with a step size of 1 s. The simulation results are shown in Figures 19–23.

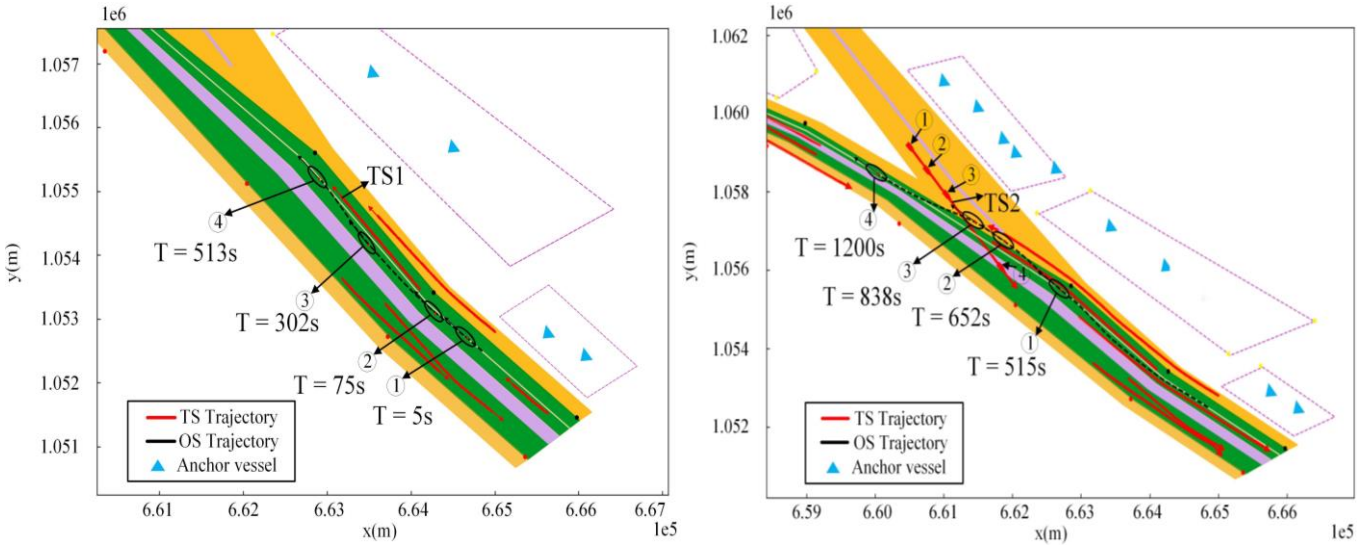

Fig. 19 Simulation experiment from 1 s to 1200 s

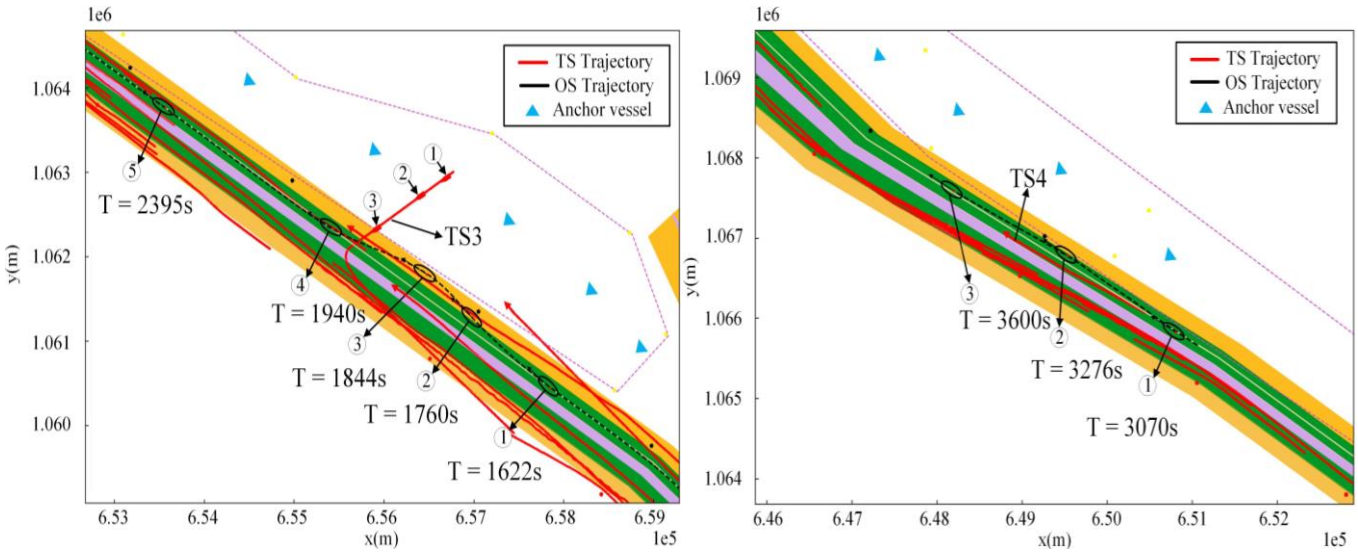

Fig. 20 Simulation experiment from 1622 s to 3600 s

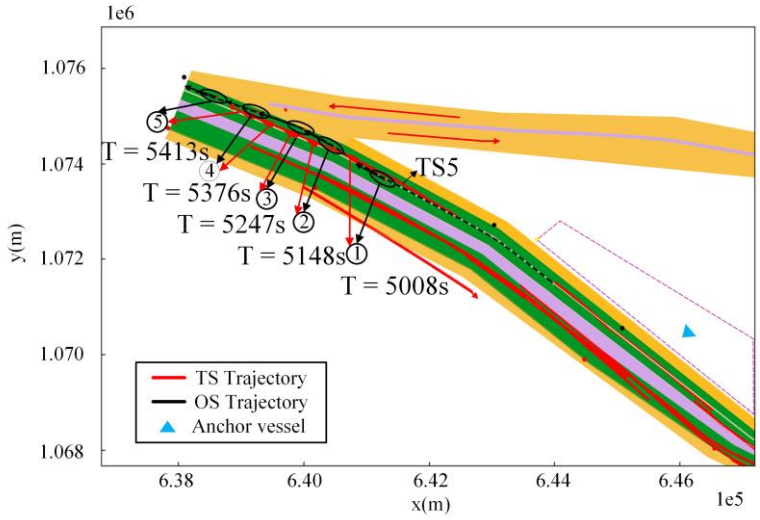

Fig. 21 Simulation experiment from 5008 s to 5413 s

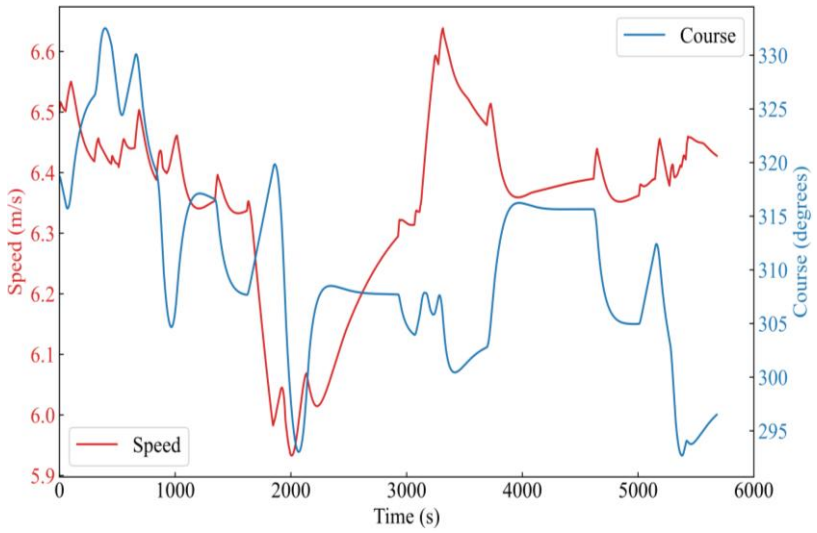

Fig. 22 Simulation experiment of the own-ship (OS) course and speed

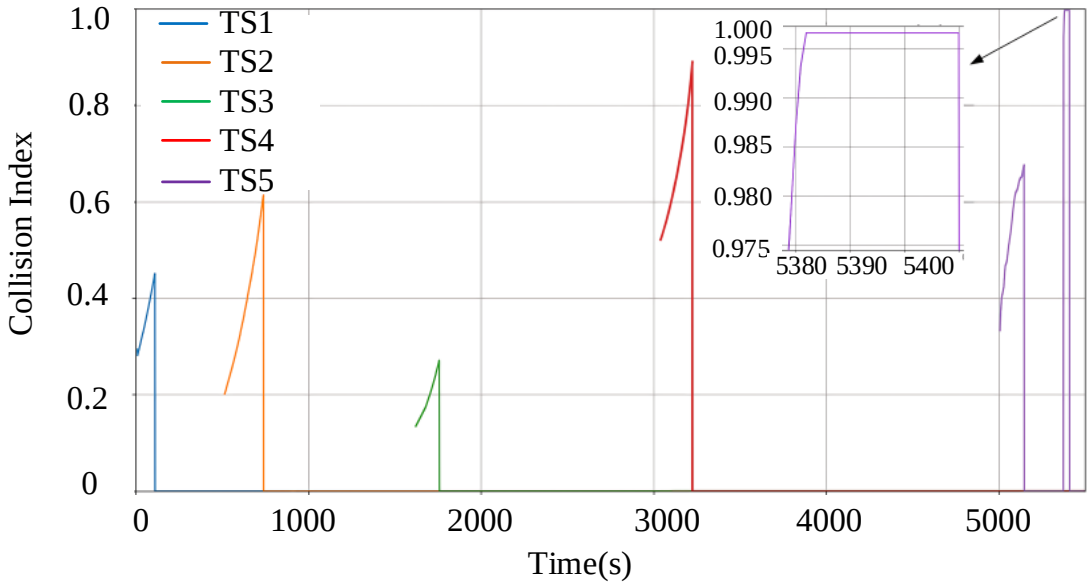

Fig. 23 Simulation of experimental collision risk index (CRI) changes

Figure 19 illustrates the simulation experiment from 1s to 1200 s. At T = 5 s, a danger was identified, marking an overtaking situation. To avoid a collision, the OS adjusted its course by 5° to port. At T = 75 s, the OS altered its course by 11° to starboard to align with the recommended traffic flow. At T = 302 s, the OS made a further course adjustment of 22° to starboard, after determining that it was safe to continue tracking the route. At T = 515 s, danger was detected, and the CRI for TS2 exceeded 0.2, indicating a branching estuary. The OS changed its course by 5° to starboard to avoid a collision. At T = 652s, the OS adjusted its course by 12° to port to follow the traffic flow recommendation. At T = 838 s, a further course change of 38° to port was made after confirming the safety of the route.

Figure 20 shows the simulation experiment from 1622 s to 3600s. At T = 1622s, a danger was calculated, indicating a traverse situation. To avoid a collision, the OS altered its course by 5° to starboard and reduced speed from full ahead to half ahead. At T = 1755 s, the OS changed its course by 5° to starboard to follow the traffic flow. At T = 1844 s, the OS adjusted its course by 5° to port and increased speed from half ahead to full ahead after determining the route was safe. A new danger was identified at T = 3070 s, signaling another overtaking scenario. The OS altered its course by 5° to starboard to avoid collision, and at T = 3275 s, the course was adjusted by 20° to port to track the route.

Figure 21 shows the simulation experiment from 5008 s to 5413s. At T = 5008 s, a danger was identified, marking an overtaking situation. The OS adjusted its course by 5° to starboard to avoid a collision. At T = 5148 s, the OS altered its course by 13° to port to align with the recommended traffic flow. At T = 5274 s, the course was adjusted by 29° to port to track the route. Danger was detected again at T = 5375 s, leading to a 5° starboard adjustment to avoid a collision. Finally, at T = 5413 s, the OS altered its course by 3° to stay on the planned route.

The course and speed of the OS throughout the voyage are shown in Figure 23. The OS could navigate safely in wide inland waterways by changing course, changing speed, and adopting a combination of changing course and changing speed.

Figure 22 depicts the change in CRI between the OS and dangerous TS in this simulation experiment. The CRI of TS5 was reduced to 0 at 5148 s, due to the collision-avoidance decision. Although the CRI increased sharply until 5375 s, it remained <1. This was because TS5 was driven by AIS data and did not consider the motion state of the OS. At this time, the situation involved overtaking TS5, which was close to the OS, creating a collision risk and causing the CRI to approach 1. However, it did not enter the OS ship domain. The subsequent maneuvering decision also reduced the CRI to 0.

6. Conclusion and future prospects

A course and speed control system was established by constructing a situational awareness model to solve the navigation decision-making problem for a channelized system of wide inland waters. By considering the water environment, navigation rules, constraints of good seamanship, and closed-loop concept of time-sequence rolling, a variable-speed navigation decision-making method for wide inland waters was proposed. This method takes the time-varying dynamic and static environmental information of the waters as the input to the decision-making framework, and through the constructed situational awareness model and navigation decision-making method, based on the principle of time-sequence rolling optimization and fast calculation, dynamically adapts to the residual error of the system and the random motion of the target ship, and calculates the navigation risk and the maneuvering decision that conforms to the good seamanship and navigation rules in real-time. Simulation experiments were conducted using real-time AIS data. The results of the experiments showed that it could effectively ensure the safety of ship navigation and track the route in time.

However, despite its promising theoretical results, this approach primarily focuses on simulations, leaving several critical practical challenges unexplored. In practical applications, navigation systems often face issues like system latency, sensor errors, and data communication delays, which could impact the timeliness and accuracy of decision-making. Sensor inaccuracies, including GPS drift or radar interference, could compromise situational awareness, potentially leading to incorrect navigation decisions. Moreover, this system does not currently account for unavoidable emergencies, including sudden mechanical failures, engine

loss of control, or situations requiring rapid deceleration or reversing. Addressing these issues is imperative for ensuring the effectiveness and reliability of the system in real-world applications. Additionally, this study does not consider the potential coupling effects of shallow water, wind, and current interactions, which can significantly influence a ship's maneuverability, especially in narrow or shallow inland waterways. Real-world conditions often involve complex, nonlinear interactions between environmental factors and ship dynamics, which are difficult to replicate in simulations fully. Incorporating these factors into the model would enhance its applicability and accuracy in real-world navigation scenarios.

Future research ought to focus on extending the adaptability of the proposed method to various waterway types and navigational environments. Exploring its performance in diverse conditions-such as varying traffic densities, different geographic regions, and dynamic weather patterns-would provide a more comprehensive understanding of its practical limitations and potential improvements. Augmenting the model's capability to integrate data from heterogeneous sources, such as weather forecasts, real-time ship behavior, and historical navigation data, could improve its decision-making accuracy and robustness. Meanwhile, future work must explore the development of an integrated testbed that combines simulation with real-world experimentation. Such an approach would enable the evaluation of system performance under realistic conditions, providing valuable feedback for improving the model and ensuring its practical effectiveness. By addressing these practical challenges and extending the model's adaptability, the proposed approach can be developed into a reliable tool for autonomous navigation and collision avoidance in inland waters, contributing substantially to the safety and efficiency of maritime transportation.

Acknowledgments

The authors acknowledge the support from the National Key R&D Program of China (Grant No. 2023YFE0203700) and National Natural Science Foundation of China (Grant numbers: 52071249, 52271367).

REFERENCES

[1] Zhao, C., Li, R., Wang, Y., Yu, H., Gong, Y., 2021. Study on the propagation of sustainable development concept among Gulf ports based on complex network. *Maritime Policy & Management*, 48(4), 478-496. https://doi.org/10.1080/03088839.2020.1783466

[2] Xie, C., Huang, L., Wang, R., Deng, J., Shu, Y., Jiang, D., 2022. Research on quantitative risk assessment of fuel leak of LNG-fuelled ship during lock transition process. *Reliability Engineering & System Safety*, 221, 108368. https://doi.org/10.1016/j.ress.2022.108368

[3] Wu, Z., Woo, S. H., Lai, P. L., Chen, X., 2022. The economic impact of inland ports on regional development: Evidence from the Yangtze River region. *Transport Policy*, 127, 80-91. https://doi.org/10.1016/j.tranpol.2022.08.012

[4] Wu, N., 2010. Fully understanding some characteristics of inland river ship collision accidents. *Navigation of China*, 33, 79-84.

[5] Mostefa, M., Krzysztof, K., Abdellah, K., 2021. Artificial Intelligence-Based Methods for Decision Support to Avoid Collisions at Sea. *Electronics*, 10(19): 2360-2360. https://doi.org/10.3390/electronics10192360

[6] Wang, Y., Zhang, Y., Zhao, H., Wang, H., 2022. Assessment method based on AIS data combining the velocity obstacle method and Pareto selection for the collision risk of inland ships. *Journal of Marine Science and Engineering*, 10(11), 1723. https://doi.org/10.3390/jmse10111723

[7] Ke, Z., Liwen, H., Xiao, L., He Y., 2022. A Novel Decision Support Methodology for Autonomous Collision Avoidance Based on Deduction of Manoeuvring Process. *Journal of Marine Science and Engineering*, 10(6), 765-765. https://doi.org/10.3390/jmse10060765

[8] Zhao, X., Huang, L., Zhang, K., Mou, J., Yu, D., He, Y., 2024. Dynamic Adaptive Decision-Making Method for Autonomous Navigation of Ships in Coastal Waters. *IEEE Transactions on Intelligent Transportation Systems*, 25(11), 17917-17930 https://doi.org/10.1109/TITS.2024.3419046

[9] Huang, Y., Chen, L., Negenborn, R. R., Van Gelder, P. H. A. J. M., 2020. A ship collision avoidance system for human-machine cooperation during collision avoidance. *Ocean Engineering*, 217, 107913. https://doi.org/10.1016/j.oceaneng.2020.107913

[10] Li, M., Mou, J., Chen, P., Rong, H., Chen, L., van Gelder, P. H. A. J. M., 2022. Towards real-time ship collision risk analysis: An improved R-TCR model considering target ship motion uncertainty. *Reliability Engineering & System Safety*, 226, 108650. https://doi.org/10.1016/j.ress.2022.108650

[11] Chen, P. F., Van Gelder, P. H. A. J. M., Mou, J. M., 2019. Integration of elliptical ship domains and velocity obstacles for ship collision candidate detection. *TransNav: International Journal on Marine Navigation and Safety of Sea Transportation*, 13(4), 751-758. https://doi.org/10.12716/1001.13.04.07

[12] Huang Y, van Gelder P. H. A. J. M., Wen Y., 2018. Velocity obstacle algorithms for collision prevention at sea. *Ocean Engineering*, 151, 308-321. https://doi.org/10.1016/j.oceaneng.2018.01.001

[13] Zhao, X., He, Y., Huang, L., Mou, J., Zhang, K., Liu, X., 2022. Intelligent collision avoidance method for ships based on COLRGEs and improved velocity obstacle algorithm. *Applied Sciences*, 12(18), 8926. https://doi.org/10.3390/app12188926

[14] Tsou, M. C., 2016. Multi-target collision avoidance route planning under an ECDIS framework. *Ocean Engineering*, 121, 268-278. https://doi.org/10.1016/j.oceaneng.2016.05.040

[15] Ni, S., Liu, Z., Cai, Y., Gao, S., 2020. Coordinated anti-collision path planning algorithm for marine surface vessels. *IEEE Access*, 8, 160825-160839. https://doi.org/10.1109/ACCESS.2020.3021091

[16] Ni, S., Liu, Z., Cai, Y., 2019. Ship manoeuvrability-based simulation for ship navigation in collision situations. *Journal of Marine Science and Engineering*, 7(4), 90. https://doi.org/10.3390/jmse7040090

[17] Ni, S., Liu, Z., Cai, Y., Wang, X., 2018. Modelling of ship's trajectory planning in collision situations by hybrid genetic algorithm. *Polish Maritime Research*, 25(3), 14-25. https://doi.org/10.2478/pomr-2018-0092

[18] Tang, J., Liu, G., Pan, Q., 2021. A review on representative swarm intelligence algorithms for solving optimization problems: Applications and trends. *IEEE/CAA Journal of Automatica Sinica*, 8(10), 1627-1643. https://doi.org/10.1109/JAS.2021.1004129

[19] Zhao, L., Roh, M. I., Lee, S. J., 2019. Control method for path following and collision avoidance of autonomous ship based on deep reinforcement learning. *Journal of Marine Science and Technology*, 27(4), 1. https://doi.org/10.6119/JMST.201908_27(4).0001

[20] Zhao, L., Roh, M. I., 2019. COLREGs-compliant multiship collision avoidance based on deep reinforcement learning. *Ocean Engineering*, 191, 106436. https://doi.org/10.1016/j.oceaneng.2019.106436

[21] Sawada, R., Sato, K., Majima, T., 2021. Automatic ship collision avoidance using deep reinforcement learning with LSTM in continuous action spaces. *Journal of Marine Science and Technology*, 26(2), 509-524. https://doi.org/10.1007/s00773-020-00755-0

[22] Shen, H., Hashimoto, H., Matsuda, A., Taniguchi, Y., Terada, D., Guo, C., 2019. Automatic collision avoidance of multiple ships based on deep Q-learning. *Applied Ocean Research*, 86, 268-288. https://doi.org/10.1016/j.apor.2019.02.020

[23] Fan, A., Wang, Z., Yang, L., Wang, J., Vladimir, N., 2021. Multi-stage decision-making method for ship speed optimisation considering inland navigational environment. P*roceedings of the Institution of Mechanical Engineers, Part M: Journal of Engineering for the Maritime Environment*, 235(2), 372-382. https://doi.org/10.1177/1475090220982414

[24] Wu, B., Cheng, T., Yip, T. L., Wang, Y., 2020. Fuzzy logic based dynamic decision-making system for intelligent navigation strategy within inland traffic separation schemes. *Ocean Engineering*, 197, 106909. https://doi.org/10.1016/j.oceaneng.2019.106909

[25] Ma, Q., Wang, Z., Zhou, T., Liu, Z., 2024. Robust optimization method of emergency resource allocation for risk management in inland waterways. *Brodogradnja*, 75(1), 1-22. https://doi.org/10.21278/brod75103

[26] Cheng, T., Wu, Q., Wu, B., Yan, X., 2021. A probabilistic decision-making system for joining traffic lanes within an inland traffic separation scheme. *Marine Technology Society Journal*, 55(5), 44-63. https://doi.org/10.4031/MTSJ.55.5.14

[27] Topçu, O., 2017. Using situational awareness for adaptive decision making in agent-based simulation. *Winter Simulation Conference*, 3-6 December, Las Vegas, Nevada, United States, 1276-1287. https://doi.org/10.1109/WSC.2017.8247873

[28] Gao, J., Zhang, Y., 2024. Ship collision avoidance decision-making research in coastal waters considering uncertainty of target ships. *Brodogradnja*, 75(2), 1-16. https://doi.org/10.21278/brod75203

[29] Yu, D., He, Y., Zhao, X., Chen, J., Liu, J., Huang, L., 2023. Dynamic adaptive autonomous navigation decision-making method in traffic separation scheme waters: A case study for Chengshanjiao waters. *Ocean Engineering*, 285, 115448. https://doi.org/10.1016/j.oceaneng.2023.115448

[30] He, Y., Du, Z., Huang, L., Yu, D., Liu, X., 2023. Maneuver Decision-Making Method for Ship Collision Avoidance in Chengshantou Traffic Separation Scheme Waters. *Applied Sciences*, 13(14), 8437. https://doi.org/10.3390/app13148437

[31] Hajizadeh, S., Seif, M. S., Mehdigholi, H., 2016. Evaluation of planing craft maneuverability using mathematical modeling. *Brodogradnja*, 67(1), 85-100. https://dx.doi.org/10.21278/brod67105

[32] Yu, Z., Amdahl, J., 2016. Full six degrees of freedom coupled dynamic simulation of ship collision and grounding accidents. Marine Structures, 47, 1-22. https://doi.org/10.1016/j.marstruc.2016.03.001

[33] Xia, Y., Zheng, S., Yang, Y., Qu, Z., 2018. Ship Maneuvering Performance Prediction Based on MMG Model. *IOP Conference Series: Materials Science and Engineering*, 15-16 September, Melbourne, Australia, 452(4), 042046. https://doi.org/10.1088/1757-899X/452/4/042046

[34] Wang, Y., Du, W., Li, G., Li, Z., Hou, J., Hu, H., 2022. Efficient Ship Maneuvering Prediction with Wind, Wave and Current Effects. *Advances in Transdisciplinary Engineering*, IOS Press. https://doi.org/10.3233/ATDE220115

[35] Lin, B., Zheng, M., Han, B., Chu, X., Zhang, M., Zhou, H., Ding, S., Wu, H., Zhang, K., 2024. PSO-Based Predictive PID-Backstepping Controller Design for the Course-Keeping of Ships. *Journal of Marine Science and Engineering*, 12(2), 202. https://doi.org/10.3390/jmse12020202

[36] Li, Y., Tang, Z., Gong, J., 2023. The effect of PID control scheme on the course-keeping of ship in oblique stern waves. *Brodogradnja*, 74(4), 155-178. https://doi.org/10.21278/brod74408

[37] Liu, J., Huang, L., Yu, D., Xu, L., He, Y., 2024. The control method for ship tracking when navigating through narrow and curved sections. *Applied Ocean Research*, 145, 103943. https://doi.org/10.1016/j.apor.2024.103943

[38] Zaman, B., Marijan, D., Kholodna, T., 2023. Interpolation-Based Inference of Vessel Trajectory Waypoints from Sparse AIS Data in Maritime. *Journal of Marine Science and Engineering*, 11(3), 615. https://doi.org/10.3390/jmse11030615